

[†]Present address: University of Alaska, College, Alas.

[‡]Present address: Dornier GmbH, P.O. Box 317, Friedrichshafen (Bodensee), West Germany.

¹R. A. Buckingham and A. Dalgarno, Proc. Roy. Soc. (London) A213, 327 (1952).

²E. E. Benton, E. E. Ferguson, F. A. Matsen, and W. W. Robertson, Phys. Rev. 128, 206 (1962).

³R. D. Poshusta and F. A. Matsen, Phys. Rev. 132, 307 (1963).

⁴F. A. Matsen and D. R. Scott, Quantum Theory of Atoms, Molecules, and the Solid State (Academic Press Inc., New York, 1966), p. 133.

⁵D. J. Klein, E. M. Greenawalt, and F. A. Matsen, J. Chem. Phys. 47, 4820 (1967).

⁶H. L. Richards and E. E. Muschlitz, Jr., J. Chem. Phys. 41, 559 (1964).

⁷E. W. Rothe, R. H. Neynaber, and S. M. Trujillo, J. Chem. Phys. 42, 3310 (1965).

⁸W. A. Fitzsimmons, N. F. Lane, and G. K. Walters, Phys. Rev. 174, 193 (1968).

⁹M. A. Biondi, Phys. Rev. 83, 653 (1951).

¹⁰E. Ebbinghaus, Ann. Phys. (Leipzig) 7, 267 (1930).

¹¹F. D. Colegrove, L. D. Scheerer, and G. K. Walters, Phys. Rev. 135, A353 (1964).

¹²P. L. Pakhomov and I. Ya. Fugol, Dokl. Akad. Nauk USSR 179, 813 (1968) [English transl.: Soviet Phys. - Doklady 13, 317 (1968)].

¹³R. A. Buckingham and A. Dalgarno, Proc. Roy. Soc. (London) A213, 506 (1952).

¹⁴S. A. Evans and N. F. Lane, Bull. Am. Phys. Soc. 14, 262, (1969).

¹⁵N. G. Utterback, Phys. Rev. Letters 12, 295 (1964).

¹⁶M. Hollstein, D. C. Lorents, and J. R. Peterson, Bull. Am. Phys. Soc. 13, 197 (1968).

¹⁷M. Hollstein, D. C. Lorents, and J. R. Peterson, Bull. Am. Phys. Soc. 14, 262 (1968).

¹⁸M. Hollstein, D. C. Lorents, J. R. Peterson, and J. R. Sheridan, Can. J. Chem. 47, 1858 (1969).

¹⁹J. R. Sheridan and J. R. Peterson, J. Chem. Phys. 51, (1969).

²⁰J. R. Peterson and D. C. Lorents, Phys. Rev. 182, 152 (1969).

²¹Excitation of the 3^3D state could result via cascade from an excitation by 2^1S atoms of the 4^1F state which mixes with the 4^3F state. The 3^1D state could be similarly excited by 2^3S atoms. However, the experimental results indicate that these processes do not contribute significantly.

²²D. R. Bates, Discussions Faraday Soc. 33, 7 (1962).

²³D. R. Bates and R. McCarroll, Advan. Phys. 11, 39 (1962).

²⁴F. J. Smith, Phys. Letters 20, 271 (1966).

²⁵J. M. Peek, T. A. Green, J. Perel, and H. H. Michels, Phys. Rev. Letters 20, 1419 (1968).

²⁶R. E. Olson, Phys. Rev. 187, 153 (1969).

²⁷R. E. Olson (private communication).

²⁸S. A. Evans and N. F. Lane, Phys. Rev. (to be published).

Rotational Excitation of the (H, H₂) System

K. T. Tang

Department of Physics, Pacific Lutheran University, Tacoma, Washington 98447

(Received 26 May 1969)

An analytic two-body potential, consistent with all available data, is presented for the (H, H₂) system. This potential is then used in the calculation of rotational excitation with the distorted-wave Born approximation. As compared with the results of previous studies, the differential cross sections are drastically different, and the total cross sections are smaller by an order of magnitude. This is because the potential used is different from that used previously.

I. INTRODUCTION

The rotational excitation of hydrogen molecules by the impact of hydrogen atoms has received considerable attention.¹⁻³ It is physically interesting because it is involved in a variety of relaxation processes,⁴ possibly including the cooling of interstellar clouds.⁵ Furthermore, it serves

as the prototype of the inelastic scattering of molecules by heavy neutral particles.

An exact solution of this many-body problem requires one to consider both the nuclei and the electrons. However, for thermal-energy collisions ($\lesssim 1$ eV), the Born-Oppenheimer approximation separating nuclear and electronic motion is valid, and a single electronic eigenfunction can

be used to represent the state of the electrons throughout the atom-molecule encounter. In the case where the translational energy is well below the first vibrational level, the problem is usually regarded as the scattering of a particle by a rigid rotator with a two-body potential.

The problem is formidable even after such simplifications. First, we must know the inter-nuclear potential provided by the solution of the electronic problem for stationary nuclei. Then the dynamics of the scattering must be obtained by solving the Schrödinger equation. Both aspects of the problem have been discussed extensively,⁶ neither of them is amenable to exact mathematical treatment.

Although we probably know more about the interactions between a hydrogen atom and a hydrogen molecule than that of any other atom-molecule system, *a priori* determination of the potential for an arbitrary configuration is not yet available. All potentials previously used in connection with the rotational excitation of this system are similar. While they yield a reasonable total cross section in the low-energy range ($\lesssim 1$ eV), the elastic cross section derived from them is much too large when compared with the experimental data of high-energy (200-800 eV) scattering.⁷ These potentials are based on the results obtained from simple perturbation calculations with 1s wave functions on the three hydrogen atoms. These wave functions lead to an energy surface which will give much too small a cross section for reactive scattering.⁸ Furthermore, the anisotropic part of these potentials which are responsible for the inelastic scattering are contradictory to all the semiempirical energy surfaces based on valence bond formulation of the polyatomic system.

Once the interaction potential is determined, the dynamic problem can be expressed in many different mathematic forms.⁹⁻¹¹ To carry out the calculation, approximation of one kind or the other has to be introduced. However, the inaccuracy caused by the approximation methods are far less than that caused by the uncertainty of the potential. For rotational excitations with low-incident energies, the distorted-wave Born approximation is generally adequate.

In this paper, we present a two-body potential which is consistent with all available data. This potential is then used to calculate the rotational excitation. As compared with the results of previous works, the total cross sections are much smaller, and the angular distributions are also significantly different.

II. INTERACTION POTENTIAL

The three-body potential of the atom-molecule system is a function of \vec{R} , the coordinate of the

atom relative to the c. m. of the molecule, and \vec{r} , the internal coordinate of the molecule. Making a harmonic analysis of the potential, we can write

$$V(\vec{R}, \vec{r}) = \sum_n V_n(R, r) P_n(\cos \chi), \quad (2.1)$$

where χ is the angle between \vec{R} and \vec{r} , and P_n is the Legendre polynomial of order n . Since H₂ is a homonuclear molecule, only even- n terms contribute. Generally, for rotational excitation at thermal-energy range, r is taken to be the equilibrium distance r_e of the molecule, and the harmonics higher than the second order are neglected. (See Sec. VI.)

There are two sets of first-order perturbation calculations for the potential, one by Margenau,¹² and the other by Mason and Hirschfelder.¹³ They used 1s wave functions on the three hydrogen atoms and approximated the exchange integrals. Margenau's results have been summarized by Takayanagi¹ into the first two harmonics (a. u. are used throughout this paper):

$$V_0(R) = 1.0 \times 10^{-4} \exp[-1.87(R - 6.3)] \\ - 2.0 \times 10^{-4} \exp[-0.935(R - 6.3)], \quad (2.2a)$$

$$V_2(R) = 0.26 \times 10^{-4} \exp[-1.87(R - 6.3)]. \quad (2.2b)$$

The results of Mason and Hirschfelder were joined to the long-range van der Waals interactions by Dalgarno, Henry, and Roberts,² to give

$$V_0(R) = 511.1 \exp(-1.9R) - 252/R^6, \quad (2.3a)$$

$$V_2(R) = 346.7 \exp(-2.0R) - 27.9/R^6. \quad (2.3b)$$

These two sets of expressions give similar numerical values except at very large distances, where Eqs. (2.3) give the correct R^{-6} dependence. These are the potentials used in the previous study of rotational excitations.

Independent of the perturbation calculations, there is a long history of theoretical attempts to obtain the three-body potential $V(\vec{R}, \vec{r})$ of the H₃ system.^{14, 15} Many approaches have been proposed; most of them employ the London formula¹⁶ and related refinements. Up to the present, the available methods are not sufficiently developed to obtain an *a priori* potential surface, and empirical data of one kind or the other have had to be introduced. Consequently, they are called semiempirical surfaces. Although there are quantitative differences among various semiempirical surfaces, all of them predict that if the distances r and R are fixed, among all configurations the potential energy is maximum when r and R are per-

pendicular ($\chi = 90^\circ$). This is just the reverse of what Eq. (2.2) or (2.3), predict. There, the second harmonic $V_2(R)$ is positive which means the energy is maximum for linear geometry ($\chi = 0$) and minimum for the perpendicular case ($\chi = 90^\circ$). Furthermore, when we make a harmonic analysis of the semiempirical energy surface, and set r equal to r_e , we find that $V_0(R)$ is much smaller than the corresponding term in either Eq. (2.2) or (2.3).

In a previous paper,¹⁷ we have constructed two-body potentials from such a potential energy surface. That surface has been used for extensive quantum¹⁸ and classical¹⁹ calculations of elastic and reactive scattering. The results are in general agreement with available data. The Legendre polynomial expansion [Eq. (2.1)] with $r = r_e$ for this potential surface is shown in Fig. 1. The results of the perturbation calculation [Eq. (2.3)] are also included in the figure for comparison. The differences between them are rather drastic.

Equations (2.2) and (2.3) are analytic expressions, so they give the potential everywhere in space [Eq. (2.3) must be cut off at small distances, since the potential goes to $-\infty$ as R approaches zero]. However, the available perturbation results that these equations are based on are limited to large distances of separation. In particular, in the region between $R \lesssim 5$ and $R \gtrsim 1$ a.u., there is no information from the perturbation calculation.

This region is where the reaction takes place. The semiempirical potential surfaces are constructed for precisely this purpose. Since the

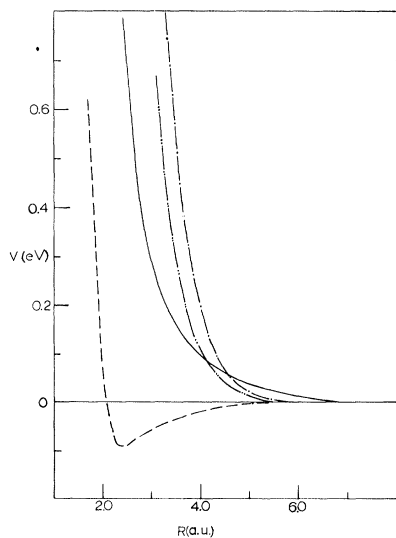


FIG. 1. Comparison of semiempirical and perturbation potentials. —, semiempirical $V_0(R)$; ----, semiempirical $V_2(R)$; - · - · - ·, perturbation $V_0(R)$; and — · — · — ·, perturbation $V_2(R)$.

semiempirical surface yields a reasonable cross section for reactive scattering,¹⁸ and agrees with the results of high-energy elastic scattering data,¹⁷ it is likely that the semiempirical calculation is close to the correct potential.

In the outer region, it is almost certain that the potential expressed in Eqs. (2.3) is more accurate. There, the two sets of perturbation calculations agree with each other. Furthermore, it has the proper van der Waals attraction, whereas the semiempirical potential is purely repulsive.

Making use of these observations, we adopt an analytic potential which agrees with the semiempirical calculation in the inner region and with the perturbation calculation in the outer region. It has the form

$$V_0(R) = 90.2 \exp[-0.617R + 1.234]/R^4 - 251.6/R^6, \quad (2.4a)$$

$$V_2(R) = 92.04 \exp[-1.87R] - 12.92 \\ \times \exp[-0.26R^2 - 0.39R] \quad (2.4b)$$

This potential is shown in Fig. 2, together with the perturbation potential of Eq. (2.3). The outer region of the potentials is illustrated in Fig. 2(b). As compared with Fig. 1, the spherical symmetric part is essentially the same as that of the semiempirical potential in the inner region. Due to the van der Waals attraction, the present potential is considerably softer for $R \gtrsim 3$ a.u. It drops to zero at about the same place ($R \approx 6$ a.u.), where the perturbation potential does. After reaching a negative minimum it approaches zero again with the appropriate R^{-6} behavior. For $R \gtrsim 7$ a.u., it is essentially identical with the potential of Eq. (2.3a).

The features of the anisotropic term $V_2(R)$ is of particular significance for rotational excitation. As shown in Fig. 1, $V_2(R)$ of the perturbation potential is positive for distances up to $R \approx 7.2$ a.u., while $V_2(R)$ of the semiempirical potential is positive only for very small distances, and for distances of practical interest ($R \gtrsim 2$ a.u.), it is negative. In the present potential, $V_2(R)$ [Eq. (2.4b)] drops from positive to negative at $R \approx 2$ a.u. essentially in the same way as the semiempirical potential does. After the minimum, it starts to rise somewhat more rapidly than the semiempirical potential. At about $R = 3.7$ a.u., it becomes positive. It reaches a maximum at $R \approx 4.4$ a.u. and approaches the perturbation potential Eq. (2.3b) at $R \approx 6.4$ a.u. At very large distances ($R \gtrsim 7.2$ a.u.), the potential of Eq. (2.3b) becomes negative, while Eq. (2.4b) does not have the same R^{-6} dependence and stays positive. However, at such distances, the absolute values of V_2 are so small ($\lesssim 10^{-4}$ eV) that little difference will be made in the cross section if Eq. (2.4b) is truncated and the tail of Eq. (2.3b) is joined to it. To compro-

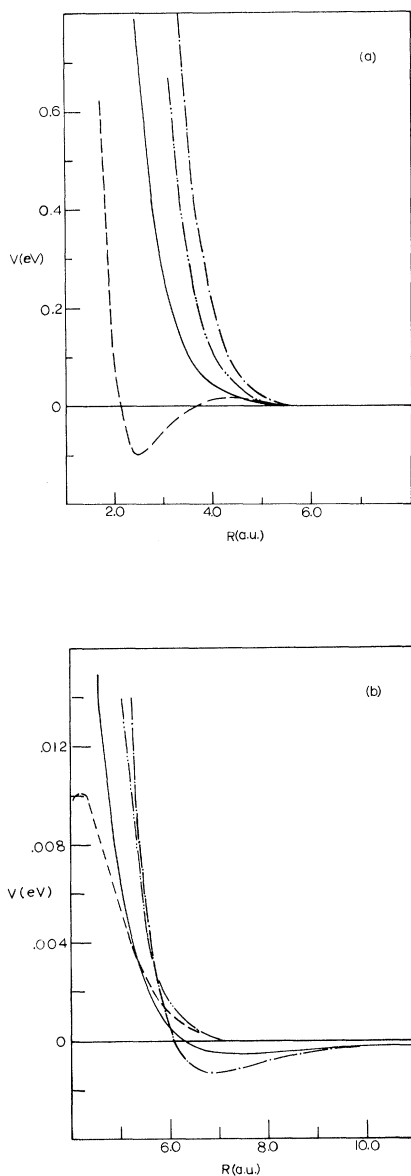


FIG. 2. Comparison of potentials of present work [Eqs. (2.4)] and that of Dalgarno, Henry, and Roberts [Eqs. (2.3)]. (a) Inner region. (b) Outer region. ——— $V_0(R)$ of Eqs. (2.4); - - - - $V_2(R)$ of Eqs. (2.4); - · - · - $V_0(R)$ of Eqs. (2.3); · · · · · $V_2(R)$ of Eqs. (2.3).

mise the semiempirical calculation and the perturbation calculation, the sign of $V_2(R)$ has to be changed twice in the important range between $R \geq 1.6$ and $R \leq 7.0$ a. u. This reversal of anisotropy, as distance of separation increases, is in agreement with recent theoretical calculations.²⁰

III. FORMULATION

To consider the inelastic scattering of a particle A by a rigid rotator BC , we write the total Hamiltonian H in the form

$$H = H_0(\vec{R}, \vec{r}) + V(\vec{R}, \vec{r}), \quad (3.1)$$

where $H_0(\vec{R}, \vec{r})$ is the noninteracting Hamiltonian of the free particle and the free rotator. The plane-wave solutions of $H_0(\vec{R}, \vec{r})$ with total energy E are (normalized to unit density)

$$\Phi_n(\vec{R}, \vec{r}) = \exp(i\vec{k}_n \cdot \vec{R}) \eta_n(\vec{r}), \quad (3.2)$$

where \vec{k}_n is the relative wave vector of the motion such that

$$E = (\hbar^2 k_n^2 / 2\mu) + \epsilon_n, \quad (3.3)$$

with η_n and ϵ_n the n th rotational eigenfunction and eigenenergy of BC . The reduced mass of the system is denoted as μ . For the total Hamiltonian H , the solutions with energy E and outgoing (+) or incoming (-) spherical-wave boundary conditions are written $\Psi_n^{(+)}$, and $\Psi_n^{(-)}$, respectively; these functions satisfy the Lippman-Schwinger integral equations²¹

$$\Psi_n^{(\pm)} = \Phi_n + (E - H_0 \pm i\epsilon)^{-1} V \Psi_n^{(\pm)}, \quad (3.4)$$

where ϵ is a positive infinitesimal which introduces the appropriate asymptotic behavior.

The differential scattering cross section from the state n to n' can be written²²

$$\sigma_{n, n'}(\hat{k}_n) = \frac{\mu}{(2\pi\hbar^2)^2} \frac{k_{n'}}{k_n} |T_{n' n}|^2, \quad (3.5)$$

where $T_{n' n}$, the transition matrix elements, are^{22,23}

$$T_{n' n} = \langle \Phi_{n'} | V | \Psi_n^{(+)} \rangle. \quad (3.6)$$

This expression is exact. The functions and the potential V are known, therefore, the difficulty in determining $T_{n' n}$ and from it $\sigma_{nm'}(k_n')$ arises in the calculation of $\Psi_n^{(+)}$. Since the exact solution is not feasible at present, approximations have to be introduced. If $\Psi_n^{(+)}$ is replaced by the plane-wave solution Φ_n , we obtain the first Born approximation. However, the Born approximation would yield very inaccurate results in the thermal-energy range. In view of the strong repulsive barrier in the (H, H₂) system, it is a better approximation to replace the total wave function $\Psi_n^{(+)}$ by the elastic scattered wave function which is the incoming plane wave distorted by the spher-

ically symmetric part of the potential. To take account of the principle of detailed balancing, the outgoing wave must be distorted also.²⁴ This can be accomplished by making use of the fact that the potential V is naturally separated into a spherical symmetric part V_0 and an anisotropic part V' [in the present case $V' = V_2(R)P_2(\cos\gamma)$]. Let us denote $\chi_n^{(\pm)}$ to be the solutions of the Hamiltonian $H_0 + V_0$; that is,

$$\chi_n^{(\pm)} = \Phi_n + (E - H_0 \pm i\epsilon)^{-1} V_0 \chi_n^{(\pm)}. \quad (3.7)$$

Writing the transition matrix $T_{n'n}$ in the form

$$T_{n'n} = \langle \Phi_{n'} | V_0 + V' | \Psi_n^{(+)} \rangle, \quad (3.8)$$

and using Eq. (3.7) to relate $\Phi_{n'}$ and $\chi_n^{(-)}$, we have

$$\begin{aligned} T_{n'n} &= \langle \chi_{n'}^{(-)} | V_0 + V' | \Psi_n^{(+)} \rangle \\ &\quad - \langle (E - H_0 - i\epsilon)^{-1} V_0 \chi_{n'}^{(-)} \\ &\quad \times | V_0 + V' | \Psi_n^{(+)} \rangle = \langle \chi_{n'}^{(-)} | V_0 | \Psi_n^{(+)} \rangle \\ &\quad + \langle \chi_{n'}^{(-)} | V' | \Psi_n^{(+)} \rangle \\ &\quad - \langle \chi_{n'}^{(-)} | V_0 (E - H_0 + i\epsilon)^{-1} V | \Psi_n^{(+)} \rangle. \end{aligned} \quad (3.9)$$

If we combine the first and last terms on the right-hand side, $T_{n'n}$ becomes

$$\begin{aligned} T_{n'n} &= \langle \chi_{n'}^{(-)} | V_0 [1 - (E - H_0 + i\epsilon)^{-1} V] | \Psi_n^{(+)} \rangle \\ &\quad + \langle \chi_{n'}^{(-)} | V' | \Psi_n^{(+)} \rangle. \end{aligned} \quad (3.10)$$

From Eq. (3.4),

$$\Phi_n = [1 - (E - H_0 + i\epsilon)^{-1} V] \Psi_n^{(+)}.$$

Substituting into Eq. (3.10), we obtain

$$T_{n'n} = \langle \chi_{n'}^{(-)} | V_0 | \Phi_n \rangle + \langle \chi_{n'}^{(-)} | V' | \Psi_n^{(+)} \rangle. \quad (3.11)$$

For inelastic scattering, the first term is equal to zero since V_0 has no angular dependence and the initial and final rotational wave functions of BC are orthogonal. Thus,

$$T_{n'n} = \langle \chi_{n'}^{(-)} | V' | \Psi_n^{(+)} \rangle. \quad (3.12)$$

This is still exact. Now if $\Psi_n^{(+)}$ is replaced by $\chi_n^{(+)}$, we obtain the distorted-wave Born approximation (DWBA)

$$T_{n'n}(\text{DWBA}) = \langle \chi_n^{(-)} | V' | \chi_n^{(+)} \rangle. \quad (3.13)$$

It is with this approximation that the present calculation is carried out.

IV. CALCULATIONS AND RESULTS

The problem of elastic scattering from the symmetrical potential $V_0(R)$, alone, is solved with the usual partial-wave analysis, that is,

$$\begin{aligned} \chi_n^+(\vec{R}, \vec{r}) &= [(k_n R)^{-1} \sum_l (2l+1) i^l e^{i\delta_l^n} U_l(k_n R) \\ &\quad \times P_l(\cos\Theta)] \eta_n(\vec{r}), \end{aligned} \quad (4.1)$$

where $U_l(k_n R)$ is a solution of the radial equation and is normalized asymptotically to

$$U_l(k_n R) \rightarrow \sin(k_n R - \frac{1}{2}l\pi + \delta_l^n), \quad \text{as } r \rightarrow \infty. \quad (4.2)$$

The phase shifts δ_l^n are evaluated by the equation

$$\tan \delta_l^n = J_l(k_n R_0) / N_l(k_n R_0), \quad (4.3)$$

where R_0 is the node of $U_l(k_n R)$; and J_l and N_l are spherical Bessel and Neumann functions, respectively. The radial equation is solved numerically by the Runge-Kutta-Gill method.²⁵ Successive nodes of the radial solution at large distances are used in Eq. (4.3) until the phase shifts so calculated agree with each other to the desired degree of accuracy. To evaluate the matrix element of Eq. (3.13), we have to do a five-dimensional integral. Using the additional theorem of Legendre polynomials²⁶ and the properties of triple products of associate Legendre polynomials,²⁷ we can carry out the angular integration analytically. However, the radial integration has to be done numerically. In the present work, it is done by Gaussian quadratures.²⁸

The total cross sections for the excitation $H + H_2(j=0) \rightarrow H + H_2(j=2)$ are shown in Fig. 3. For comparison, the results obtained by Dalgarno, Henry, and Roberts,² using the potential of Eqs. (2.3), are also included in the figure. As is seen, there is a drastic difference between the two sets of results. At $E = 0.17$ eV, the present result is smaller by an order of magnitude. As

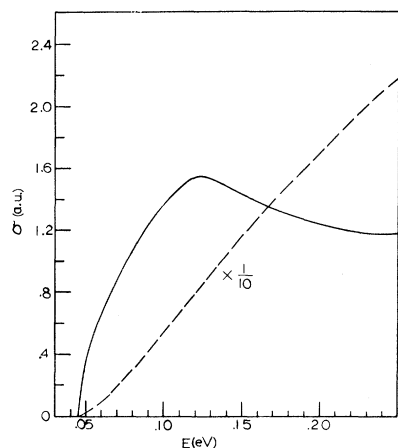


FIG. 3. Total cross section of rotational excitation from $j=0$ to $j=2$ as a function of incident energy. — results of present work, ---- results of Dalgarno, Henry, and Roberts (Ref. 2). Their results have been reduced by a factor of 10 as shown in the figure.

the energy increases, the difference between these two widens further. An interesting feature of the present result is that the total cross-section curve rises to a maximum at about $E=0.12$ eV, and then drops slowly to a minimum at about $E=0.24$ eV. After that, it rises again. On the other hand, the cross section obtained with the potential of Eqs. (2.3), as functions of energy, rises monotonically at all energies.

The differential cross sections are shown in Fig. 4 for a few incident energies. The predominant feature of these curves is the strong forward peak. As the energy increases, a small backward peak starts to appear. These results contrast sharply with that of Dalgarno, Henry, and Roberts. Their differential cross sections at different energies all have the same qualitative shape, most of the scattering occurring in the backward direction. This situation of backward scattering is not changed in the close-coupling calculations.³

To gain some insight into this behavior, we examine the individual contribution of each orbital angular momentum to the total cross section. From Eqs. (3.13) and (4.1), it is seen that the total cross section can be expressed as

$$\sigma = \sum_l (2l+1) A_l.$$

This is because the Legendre polynomials are orthogonal.

Since l (in units of \hbar) corresponds to the impact parameter b times the relative momentum P in the classical picture, and $(2l+1)$ is proportional to the area between the circle with radius $(l+1)$

and the circle with radius l , we can interpret A_l to be the relative probability of excitation for that particular l .

The A_l 's calculated from the potential of Eqs. (2.4) are shown in Fig. 5; those calculated from the potential of Eqs. (2.3) are shown in Fig. 6. These curves can be understood in terms of the corresponding potentials.

The anisotropic term $V_2(R)$ of the potential in Eq. (2.3) increases monotonically as R decreases. The deeper the incoming wave penetrates the potential, the larger is the transition matrix element which is controlled by $V_2(R)$. Because of the centrifugal potential $l(l+1)/R^2$, the penetration is less for larger l . Therefore, the probability of excitation decreases smoothly as l increases. It is also clear that for a given l , the incoming wave will penetrate deeper and yield a larger probability of excitation if its energy is higher. These features are all shown in Fig. 6.

On the other hand, $V_2(R)$ of Eqs. (2.4) changes sign twice. This makes the general behavior of the A_l , which are shown in Fig. 5, dependent on the incident energy. For $E=0.10$ eV, the incoming wave first samples the positive portion of V_2 , then samples the portion with the negative sign. The contributions from these two parts have opposite sign and compensate each other somewhat. As l increases from zero, the incoming wave is pushed outward and away from the negative part of $V_2(R)$. Thus, the probability of excitation increases. After it reaches the maximum, it finally drops to zero, since any further increase in l will put the wave completely outside the region where $V_2(R)$ is nonvanishing. As the incident energy is increased to $E=0.15$ eV, the waves

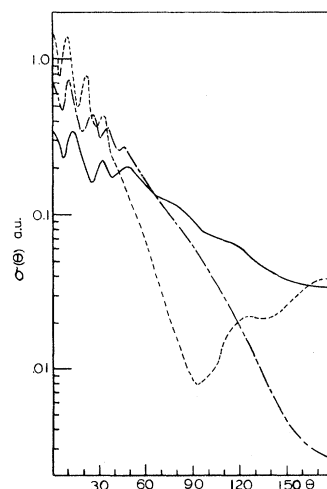


FIG. 4. Differential cross sections as a function of incident energy E . — $E=0.10$ eV; ---- $E=0.15$ eV; - · - · $E=0.25$ eV.

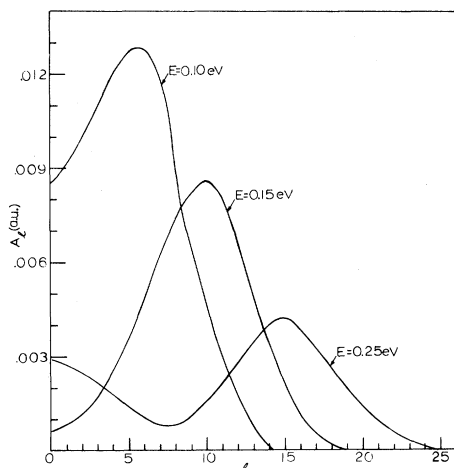


FIG. 5. Probability of excitation as a function of orbital angular momentum l calculated from the potential of this paper [Eqs. (2.4)].

with small l penetrate deeper into the potential and sample the negative part of $V_2(R)$ more. Thus, the compensation effect becomes more pronounced and the probability of excitation becomes smaller instead of larger. As l increases, A_l starts to rise and, after a maximum, falls to zero as before. When the energy is further increased to $E=0.25$ eV, the incoming wave with l equal to zero penetrates so deep that the contribution from the negative part of $V_2(R)$ overtakes the contribution from the positive part. Under this condition, when the waves are pushed out by the centrifugal potential, the contribution from the negative part becomes smaller, and closer to the contribution from the positive part. The net result is that the probability of excitation is decreased as l is increased. After it drops to a minimum at $l=7$, it starts to rise again in the same manner as other curves in the figure.

It is interesting to note that, although the overall features of the curves in Fig. 5 are very different from those in Fig. 6, the corresponding curves do have similar behavior at large l values. This is because the potentials in Eqs. (2.3) and (2.4) are almost identical for large distances of separation.

From these probability curves, we can understand both the total cross sections and the differential cross sections. The curves shown in Fig. 6 indicate that excitations can take place most easily for head-on or nearly head-on collisions. Such collisions, because of the strong repulsive core of the potential, will make the colliding system rebound in the backward direction. Thus, in the c. m. system, we expect to find a backward peak in the differential cross sections. Further-

more, since the probability increases with increasing energy for all l , the total cross section should also increase with increasing energy. These features are exactly what have been found.

The situations shown in Fig. 5 are quite different. The maximum probability of excitation does not occur at $l=0$, but at some other l . This corresponds to the scattering with some impact parameter b ($b \approx l\hbar/p$, where p is the linear momentum in the classical picture). Assuming the particles will continue their journey after the excitation has taken place, we will find a forward peak. These forward peaks in the differential cross sections are shown in Fig. 4. When the energy is increased to $E=0.5$, a secondary maxima appears at $l=0$ in the probability curve. This maxima corresponds to the small backward peak in the differential cross-section curve for $E=0.5$ in Fig. 4. We expect this backward peak to grow as the energy is increased further. The total cross section of excitation, calculated from the potential of Eqs. (2.4), increases at first, as the energy is increased. After it reaches the maximum, the compensation effect of the positive and negative part of V_2 becomes so strong that the total cross section starts to decrease. Then the negative part overtakes the positive part, and the cross section starts to rise again. Thus, the total cross-section curves shown in Fig. 3 are not unexpected. The reason the cross section calculated from the present potential are much smaller than those calculated from the perturbation potential is that the anisotropy $V_2(R)$ is much smaller in the present potential.

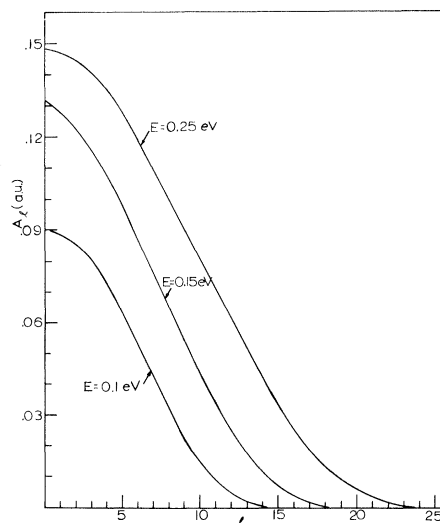


FIG. 6. Probability of excitation as a function of orbital angular momentum l calculated from the perturbation potential [Eqs. (2.3)].

V. DISCUSSION

The distorted-wave approximation has been put into a variety of mathematical forms by many authors,¹¹ although in essence they must reduce to the form of Eq. (3.13). Most existing calculations of rotational excitations^{29,30} are carried out in the formalism of Arthurs and Dalgarno,⁹ who expand the cross section in terms of the total angular momentum of the system. Without arguing the advantage or disadvantage of methods we simply evaluate the transition matrix of Eq. (3.13) with the potential [Eqs. (2.3)] that was used in the study of (H, H₂) excitation by Dalgarno, Henry, and Roberts² with that formalism. The total cross sections obtained with the present program agree well with their results. The differential cross sections also have very similar behaviors as theirs. (There are typographical errors in all their figures. Although the cross sections are labeled in the units of Å², the curves do not sum up to the values reported in the text. Nor is there a single scaling factor which can normalize all the curves in each figure to the reported values.) This can be seen by multiplying $(2l+1)$ to each l value in Fig. 6. The resulting curves have the identical shape as their Fig. 1. Therefore, it seems that there is no advantage of one method over the other, as far as numerical results are concerned.

The distorted-wave method will fail when the elements of the scattering matrix is large compared with unity. This particular problem has been investigated by Allison and Dalgarno³ with a close-coupling calculation. They used the potential of Eqs. (2.3). It is found that the departure of the distorted-wave scattering matrix from unitarity becomes serious above energies of 0.15 eV. The error of the distorted-wave approximation increases with increasing energy, at 0.25 eV, it overestimates the cross section by 50%. However, with the potential proposed in the present work [Eqs. (2.4)], the elements of the scattering matrix are much smaller. As seen in Fig. 3, the total cross sections for $E \geq 0.15$ eV obtained with the potential of Eqs. (2.4) are smaller than those obtained with the potential of Eqs. (2.3) by more than an order of magnitude. Therefore, the distorted-wave approximation may still be very accurate with the present potential. In any

case, the inaccuracy of the method is far less than that caused by the uncertainty of the potential.

For (H, H₂) excitation, there is a contribution from the rearrangement process. Since the three hydrogen atoms are indistinguishable, the wave function must obey the Pauli exclusion principle. Although this contribution can be included by the appropriate antisymmetrization procedure,¹⁸ it is neglected because the cross section of rearrangement scattering is very small.¹⁸

Both the total and differential cross sections of our calculation are drastically different from those of the previous works. This means that many relaxation processes including the cooling of the interstellar clouds in regions of neutral hydrogen should be reevaluated. Equally important, it suggests that measurements of the rotational excitation would yield useful information about the all-important H₃ potential with three particles at small distances of separation. This information is essential for a clear understanding of the fundamental exchange reaction (H + H₂ → H₂ + H). The elastic scattering is dominated by the potential tail in the outer region. The reactive cross section (if it is obtainable directly from beam experiments) would be too small to be interpreted unequivocally. Therefore, an experimental study of both the total and the differential cross sections of the inelastic scattering of this system is extremely interesting.

It must be pointed out, however, that the rigid rotator approximation of the molecule is but a zeroth-order approximation. To some extent, the initial molecule adiabatically follows the incoming atom.¹⁷ There is some exchange of energies among various degrees of freedom, with the molecule stretching and turning toward the incoming atom. The effects of adiabaticity on excitation cross sections are now under investigation.

ACKNOWLEDGMENTS

It is a pleasure to acknowledge the assistance of Dr. E. B. Moore, Jr., and Dr. C. M. Carlson. Without their help, this work would not have been possible. The author also wishes to thank Professor M. Karplus for information about his recent theoretical calculation of the H₃ potential.

¹K. Takayanagi, Proc. Phys. Soc. (London) **A70**, 348 (1957); K. Takayanagi and S. Nishimura, Publ. Astron. Soc. Japan **12**, 77 (1960).

²A. Dalgarno, R. J. W. Henry, and C. S. Roberts, Proc. Phys. Soc. (London) **88**, 611 (1966).

³A. C. Allison and A. Dalgarno, Proc. Phys. Soc. (London) **90**, 609 (1967).

⁴K. Takayanagi, Progr. Theoret. Phys. (Kyoto) Suppl. **25**, 1 (1963).

⁵L. Spitzer, Astrophys. J. **109**, 337 (1949); B. Field, W. B. Someville, and K. Dressler, Ann. Rev. Astron. Astrophys. **4**, 207 (1966).

⁶For a review, see K. Takayanagi, Advan. At. Mol. Phys. **1**, 149 (1965).

- ⁷I. Amdur, M. C. Kells, and D. E. Davenport, *J. Chem. Phys.* **18**, 1676 (1950).
- ⁸I. Shavitt, R. M. Stevens, F. Minn, and M. Karplus, *J. Chem. Phys.* **48**, 2700 (1968).
- ⁹A. M. Arthurs and A. Dalgarno, *Proc. Roy. Soc. (London)* **A256**, 540 (1960).
- ¹⁰W. H. Miller, *J. Chem. Phys.* **49**, 2373 (1968).
- ¹¹C. F. Curtiss and R. B. Bernstein, *J. Chem. Phys.* **50**, 1168 (1969), and the references therein.
- ¹²H. Margenau, *Phys. Rev.* **64**, 731 (1943); **66**, 303 (1944).
- ¹³E. A. Mason and J. O. Hirschfelder, *J. Chem. Phys.* **26**, 756; E. A. Mason and J. T. Vanderslice, *ibid.* **28**, 1070 (1958); **33**, 492 (1960).
- ¹⁴See, for example, H. J. Johnston, *Gas Phase Reaction Rate Theory* (Ronald Press Co., New York, 1966), Chap. 4.
- ¹⁵R. N. Porter and M. Karplus, *J. Chem. Phys.* **40**, 1105 (1964).
- ¹⁶F. London, *Z. Elektrochim.* **35**, 552 (1929).
- ¹⁷K. T. Tang and M. Karplus, *J. Chem. Phys.* **49**, 1676 (1968).
- ¹⁸K. T. Tang, Ph.D. thesis, Columbia University, 1965 (unpublished).
- ¹⁹M. Karplus, R. N. Porter, and R. D. Sharma, *J. Chem. Phys.* **43**, 3259 (1965).
- ²⁰M. Karplus (private communication).
- ²¹B. Lippmann and J. Schwinger, *Phys. Rev.* **79**, 469 (1950).
- ²²T. Y. Wu and T. Ohmura, *Quantum Theory of Scattering* (Prentice-Hall, Inc., Englewood Cliffs, N. J., 1962), Chap. 1; A. Messiah, *Quantum Mechanics* (John Wiley & Sons, Inc., New York, 1962), Chaps. 10 and 19.
- ²³M. L. Goldberger and K. M. Watson, *Collision Theory* (John Wiley & Sons, Inc., New York, 1964).
- ²⁴E. Wigner, in *Energy Transfer in Gases* (Wiley-Interscience, Inc., New York, 1962), p. 211.
- ²⁵S. Gill, *Proc. Cambridge Phil. Soc.* **47**, 96 (1951).
- ²⁶E. T. Whittaker and G. N. Watson, *A Course of Modern Analysis* (University of Cambridge Press, Cambridge, 1943), p. 328.
- ²⁷B. Alder, S. Fernbach, and M. Rotenberg, in *Methods in Computational Physics* (Academic Press Inc., New York, 1963), Vol. 2, p. 170.
- ²⁸F. B. Hilderbrand, *Introduction to Numerical Analysis* (McGraw-Hill Book Co., New York, 1956), Chap. 8.
- ²⁹W. D. Davison, *Proc. Roy. Soc. (London)* **A280**, 227 (1964).
- ³⁰C. S. Roberts, *Phys. Rev.* **131**, 209 (1963).

Born-Wave Calculation of Atom-Atom Inelastic Cross Sections: Excitation of He(1^1S) to He(N^1L) by Hydrogen Atoms

Hiram Levy II

Smithsonian Astrophysical Observatory, Cambridge, Massachusetts 02138

(Received 9 June 1969)

Total first Born-wave excitation cross sections are calculated for $\text{He}(1^1S) + \text{H}(1s) \rightarrow \text{He}(2^1S, 3^1S, 4^1S, 5^1S, 2^1P, 3^1P, 4^1P, 3^1D, 4^1D, 5^1D) + \text{H}(\Sigma)$ over the energy range 1.0 keV to 1.6 MeV. The highly accurate numerical generalized oscillator strengths of Kim and Inokuti and of Bell, Kennedy, and Kingston are used to describe the projectile excitations. The complete summation over target final states is performed both exactly by use of the analytic generalized oscillator strengths and approximately by use of the closure relationship. The results are compared with available experimental data and previous calculations, and the discrepancies are discussed. The differences between results calculated by summation over all the target final states and those calculated by the assumption of closure are also discussed.

I. INTRODUCTION

Paper I¹ suggested that first Born-wave direct inelastic cross sections be calculated by the use of elastic and inelastic x-ray form factors to describe the target and theoretical or experimental generalized oscillator strengths to describe particular

excitations of the projectile or target. A number of excitation and ionization cross sections for atomic hydrogen H in collisions with various target gases were calculated and compared with experimental data in order to demonstrate the effectiveness of a form-factor description of the target atom. Similar first Born calculations have